Face Identification Based on moment features

Ass.Pro.Dr.: Suhad A. Ali[1]
Babylon University/Science college for women /Computer Dep.
Email:suhad_ali2003@yahoo.com

Ass.Pro Hadab Khalid Obayes[2]
Babylon University/ College of education for human sciences
Email:hedhabsa@gmail.com

ABSTRACT :
An automatic human face recognition has been rapidly developing as one of the most active research areas of pattern recognition and computer vision due to its promising application such as personal identification automated surveillance and intelligent human computer interaction although numerous approaches have been proposed for face recognition general face identification task is still an unsolved problem. The proposed method introduces an experimental evaluation to the effectiveness of utilizing moment features in the application of face identification, where the simulation results on ORL face database show that this method obtained good results of 92%. Also, in proposed method the strength of each feature will be studied.

الملخص
تمييز الإنسان بواسطة الوجه تطور بشكل سريع وأصبح إحدى المجالات الفعالة في تمييز الأنماط والرؤيا بالحاسوب بسبب تطبيقاته المهمة مثلا نظام مراقبة الأشخاص والتفاعل الذكي بواسطة الحاسوب وان مشكلة تمييز الإنسان بواسطة الوجه قد تم تحديدها على انها وجه بشري ولكن ليس بشكل قطعي لتحديد هوية الشخص لاختلاف الاشكال من شخص الى اخر.
تم اقتراح في هذا البحث طريقه باستخدام خصائص التعجيل وتم تطبيق الطريقة المقترحة على قاعدة بيانات ORL وأوضحت النتائج كفاءة الطريقة المقترحة وكذلك تبين إن هنالك بعض الخصائص التي تمتلك قوه كبيره في التمييز أكثر من غيرها.

Keywords: SFIH, feature extraction, Nearest centroid classifier.

1.Introduction

Identity and emotion of person are conveying by the face which is become primary center of attention in the society. Although the ability to infer intelligence or character from facial appearance is suspect, the human ability to recognize faces is remarkable. A thousands of faces that human have been learned during the lifetime can be recognized, also he can recognize common faces at a glance even after years of separation. This ability is relatively strong, although of large changes in the visual motivation as a result of aging , viewing conditions, distractions such as glasses, beards or changes in hair style and expression [1].

Face recognition algorithms can be classified into two broad categories according to feature extraction schemes for face representation: feature based methods and appearance methods [2]. In feature based method, properties and geometric relations such as the areas ,distances, and angles between the facial feature points are used as descriptors for face recognition .On the other hand ,appearance based methods consider the global properties of the face image intensity pattern.

Typically appearance based face recognition algorithms proceed by computing basis vectors to represent the face data efficiently. In the next step, the faces are projected onto these vectors and the projection coefficients can be used for representing the face images[3].

Among the various biometric ID methods, the physiological methods (fingerprint, face, DNA) are more firm than methods in behavioral category (keystroke, voice print). The cause is that physiological features are often unchangeable except by severe injury. The behavioral patterns, on the other hand, may alter due to fatigue , stress, or illness. However، behavioral IDs have the advantage of being no intrusiveness. People are more comfortable signing their names or speaking to a microphone than placing their eyes before a scanner or giving a drop of blood for DNA sequencing. face recognition has drawn the attention of researchers in fields from security, psychology, and image processing, to computer vision [4]. Numerous methods have been proposed for face recognition. Some recent researches are:

- In 2013, Hamid et al., proposed a method for facial expression recognizing using texture descriptor for face image. In this method Local Binary pattern (LBP) is used for feature extraction. In the classification stage, Support Vector Machine (SVM) is used [5].
- In 2014, Joythi and Parabhakar proposed multi modal for face recognition. They used curvelet transform for features extraction stage. The K-Nearest Neighbor classifier is used to compute decision score [6].
- In 2015, K.srinivasa et al. proposed a method for texture face recognition using Local Ternary pattern (LTP) for feature extraction. A distance function is used for classifying feature vectors. This method is applied on ORL database [7].
- Samer Kais [8] proposed a method for face recognition using Discrete Cosine Transform (DCT) on face image block and Principle Component Analysis (PCA) is used on each block to reduce dimension. Then each reduced block is modeled using Hidden Markov Modal (HMM).
- S. Majumder and Devendran B. [9] using lifting schema to construct Discrete Wavelet Transform (DWT) structure. Then local

binary pattern is used for feature extraction. At last stage Euclidian distance is used for features classification.

The rest of the paper is organized as follows; section 2 present the proposed method. Section 3 gives experimental results and discussions.

2. Proposed Method

The proposed method implements the face identification system based on two stages, the first stage is *feature extraction* stage and the second stage is the *classification* stage. The feature extraction stage includes using nth order moment histogram features, while the classification stage includes using Nearest centroid classifier.

The proposal method algorithm implemented by using Delphi packages, this work is applied classifier for a face database consist of 100 face images from ORL database.

The proposed system consist of many stages as depicted in the figure (1):

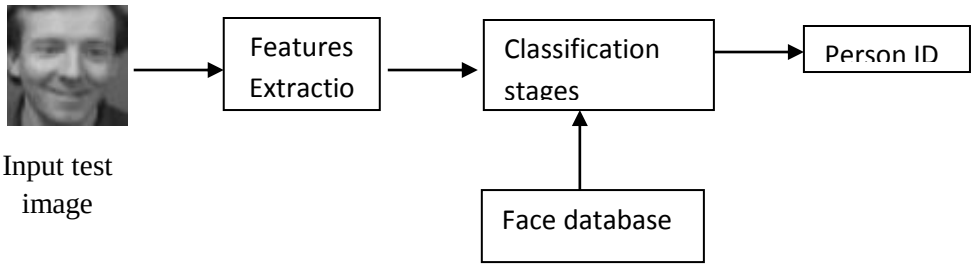

Figure (1) stages of the proposed system

2.1 Olivetti Research Laboratory (ORL) Data Base Of Face

This paper consider the well known database that taken in Cambridge UK [10].this database contains a set of faces images taken at different times, varying lighting facial expressions i.e. open and closed eyes, smile and non smiling, and facial details such as glasses or no glasses. All the images were taken against homogenous background with the subject in an upright. Figure (2) shows samples of ORL database.

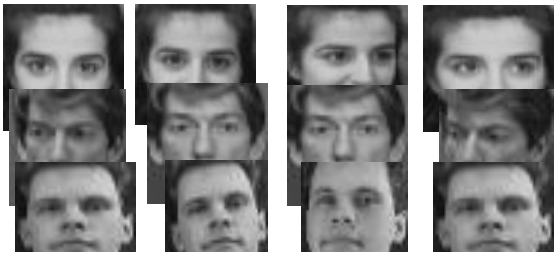

Figure (2)Samples of ORL database

2.2 Feature Extraction

One approach of texture analysis features is Statistical Frequency Intensity Histogram (SFIH). One type of measures is based on statistical moments. The equation (1) depicts the n^{th} order movements about the mean [11]:

$$\mu_n = \sum_i^{L-1} (g_i - m)^n p(g_i) \qquad \ldots\ldots\ldots (1)$$

Where g_i is a random variable referring intensity or gray level.

$P(g_i)$ is the probability of the intensity levels in the image.

L is the number of possible gray levels.

M is the average of intensity levels, which is computed according to the following equation:

$$M = \sum_{i=1}^{L-1} g_i p(g_i) \qquad \ldots\ldots\ldots\ldots\ldots\ldots (2)$$

2.3 Classification Stage

The next stage is the classification stage, and consists of using Nearest centroid classifier measurements; the goal of this stage is to find the nearest template to the input face image. In machine learning, a nearest centroid or nearest prototype classifier is a classification model that assigns to (input test face image) the label of the class of training samples whose mean (centroid) is closest to the observation.

Nearest centroid classifier is computed according to the following steps [12]:

***Step1*:** at the training stage, given labeled training samples $\{(\vec{x}_1, y_1), \ldots, (\vec{x}_n, y_n)\}$ with class labels $y_i \in \mathbf{Y}$, compute the per-class centroids according to the following equation:

$$\vec{\mu}_l = \frac{1}{|C_l|} \sum_{i \in C_l} \vec{x}_i \qquad \ldots\ldots\ldots\ldots (3)$$

where C_l is the set of indices of samples belonging to class $l \in \mathbf{Y}$.

***Step2*:** Prediction function: the input test image is assigned to a class $\vec{x}$ by measuring the Euclidian Distance between the input test image and each class template in database. The class that have minim distance will be the *ID* of input image according to the following equation:

$$\hat{y} = \arg\min_{l \in \mathbf{Y}} \left\| \vec{\mu}_l - \vec{x} \right\|. \qquad \ldots\ldots\ldots\ldots (4)$$

3. Experimental Results

In this section**,** two stages are applied in the proposed method. These are training and testing stages respectively.

3.1 Training Stage

In this stage, the features are extracted and saved in temporary file (database). The number of training images for each person is taken four images.

3.2 Testing Stage

In this stage, the enrollment image is fed to the system at first, then moment histogram features are extracted and save in features vector. At

last stage the comparison between test features vector and all saved features templates is done using Euclidian distance and the template that give smallest distance represent the *ID* of enrollment (testing) image.

In this section, the results will be review using recognition accuracy ***(R)*** parameter, which computed using the following formula:

$$R = (\frac{\text{Number of success images}}{\text{Total number of images}}) \times 100 \qquad ,\ldots\ldots\ldots \qquad (5)$$

Table (1) shows the results of attained overall recognition accuracy (R) using four training samples.

Table(1) Overall recognition accuracy for ORL database with training samples is set 4

Recognition Accuracy R (%)	Number of *n* moment features
61,458	5
86,559	25
88,542	50
90,625	80
90,625	90

It can be shown from table (1) that recognition accuracy increased as the features number increased and reach the highest value with feature number (50). As the number of training samples increased the overall recognition accuracy increased as shown in table (2).

Table(2) Overall recognition accuracy for ORL database with training samples is set 5

Recognition Accuracy R (%)	Number of *n* moment features
72	5
87	25
90	50
90	80
92	90

3.3 Discrimination Power of Each Feature

To study the effect of each feature on recognition accuracy a heuristic features analysis method is used. So, the feature vector will contain ninety elements. The discrimination power of each feature (from the ninety features) is shown in figure (3). *Four* images have been used in the training phase, while all images belong to all classes have been used in testing.

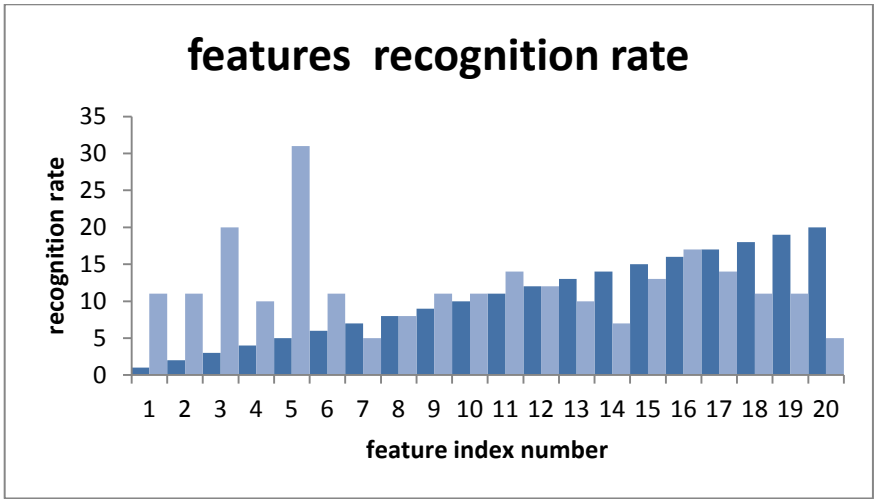

Figure (3) The discrimination power of each feature calculated for the four training images belong to ORL

As shown from figure(2) The horizontal axis in the figure represents the index number of the used feature, while the vertical axis represents the attained recognition rate. The presented results indicate that the feature with index number (5) is the best one because it led to highest recognition rate (31%), while feature number *seven* led to the lowest recognition rate (5%). The combinations of two, three, four, and ten features have been taken into account to improve the overall success rate of the recognition system. The best attained recognition rate for combinations of two features was (45%); it is met when combining features 1 & 5.

4. Conclusions and Future Works

In this paper, a new method was proposed for face identification using moments based histogram features. The proposed face identification method is relatively simple and efficient as shown from the attained results. It is found from the obtained results that:

1. image histogram proved to be good face representation media to provide discriminating features lead to good recognition accuracy.
2. It can be noted as the number of features increased, the recognition accuracy increased. Also, it can be shown from figure (3) that not all the

features effect on the recognition accuracy, where there are some features effect on recognition accuracy badly.
For future works, only the features that have strength power on accuracy results will be taken and neglected other features. Also, other texture feature sets such as GLCM (Gray Level Coocurrence Matrix) and RLM (Run Length Matrix) can be used.

References

[1] Manish K., Himanshu A. "**Face Recognition Using Eigen Faces and Artificial Neural Network**, Vol. 2, No. 4, August, 2010.

[2] Anil Jain, Patrick Flynn, Arun A. Rose, "**Handbook of Biometrics**", Springer, 2007.

[3] Gull A.B, "**Holistic Face Recognition By Dimension Reduction**", M. SC. thesis, Electrical And Electronics Engineering Department, Middle East Technical University ,2003.

[4] Aleksandra Babich, "Biometric Authentication. Types of Biometric Identifies", Bachelor's thesis, Haaga-helia university of applied science, 2012.

[5] Hamid S., Abolghasem A., and Mohamed R.," Facial Expression Recognition Using Texture Description of Displacement Image", journal of information system and telecommunication, Vol. 2, No. 4,pp. 205-212, 2014.

[6] Joythi K. and Parabhakar C. J.," **Multi Modal Face Recognition Using Block Based Curvelet Features**" international journal of computer graphics & animation, vol. 4, No. 2, pp.21-37, 2014.

[7] K.Srinivasa Reddy, V. Vijaya Kumur, and B.Eswara Reddy, " **Face Recognition Based on Texture Features using Local Ternary Patterns**" I.J. Image, Graphics and Signal Processing, vol.10, pp.37-46, 2015.

[8] Samer Kais Jameel, " **Face Recognition System Using PCA and DCT in HMM",** vol. 4, issue 1, pp. 13-18, 2015.

[9] S. Majumder and Devendran B., " **Face Recognition Using Lifting Based DWT and Local Binary Pattern**, international research journal of engineering and technology, vol.2, issue, 3,pp.830-834, 2015.

[10] At&T laboratories Cambridge database of faces. "http:/www.uk.research.att.com:pub/data/att_face.zip".

[11] S.F. Bahget, S.Ghomiemy, S. Aljahdali, M.Alotaibi," **A Proposed Hybrid Technique for Recognizing Arabic Character**", international journal of advance research in artificial intelligence, vol. 1,no 4, pp.35-42,2012.

[12] Cover T. and Hart P.," Nearest Neighbor Pattern Classification", IEEE transactions on information theory, vol. 13, issue 1, pp.21-27, 1967.

Effect of Annealing on the Structural Properties of ($Sn_{1-x}V_xO_2$) Thin Films Prepared by Chemical Spray Pyrolysis Method

Ziad. T.Khodair[1], Adnan.A.Mohammed[2]
College of Science, University of Diyala[1], Directorate-General for Education Diyala[2]

ABSTRACT

In this paper, ($Sn_{1-x}V_xO_2$) thin films, where (x = 0, 2, 4, and 6) % have been deposited on glass substrates by chemical spray pyrolysis technique (CSP) at substrate temperature of (400 ºC), thickness of about (400±10) nm and annealing temperatures (550 ºC). The structural properties of these films have been studied using XRD. XRD investigations results showed that all the films before and after annealing temperature were polycrystalline in nature with tetragonal structure and preferred orientation along (110) plane. Doping with Vanadium caused decrease the grain size before and after annealing temperature, increase of dislocation density, micro strain before and after annealing temperature.

Keywords: *SnO_2 , thin films, Annealing, Spray Pyrolysis, Structural Properties.*

1-INTRODUCTION

Tin dioxide, SnO_2, is an important n-type semiconductor, It is a tetragonal rutile structure with lattice parameters (a = b =4.737 Å) and (c = 3.826 Å) , The unit cell contains two tin and four oxygen atoms. Each tin atom is bound to six oxygen atoms at the corners of a regular octahedron, and every oxygen atom is surrounded by three tin atoms[1]. Tin oxide has been extensively investigated for gas sensors, optical-conductive coatings for solar cells [2], and electrocatalytic anodes[3], glass coatings for furnace windows as well as transparent electrodes for liquid crystal displays[4]. Tin dioxide (SnO_2) has a density of (6.95g/cm^3) and molecular weight of (150.69 g/mol). Its melting point is (2360 ºC) [5]. SnO2 films have been fabricated using various technologies such as sol-gel, spray pyrolysis, ion beam sputtering, magnetic sputtering, and pulsed laser[6]. Vanadium (V) lies with the transition metals on the periodic table,The atomic number of Vanadium is 23 with an atomic mass of 50.94 [7]. In this study we report the effect

of annealing temperature on the structural properties of ($Sn_{1-x}V_xO_2$) film.

2. EXPERIMENTAL PROCEDURE

Chemical spray pyrolysis technique was used to deposit undoped and Vanadium -doped (SnO_2) films on glass substrates at temperature of (400 ºC). A homogeneous solution was prepared by dissolving ($SnCl_4.5H_2O$) and (VCl_3) in distilled water at the concentration of 0.1 M at room temperature in which the volumetric ratios of V were (0,2,4.6,)%.The resultant solution was sprayed on glass substrate. Other deposition conditions such as spray nozzle substrate distance (30 cm), spray time (7 s), spray interval (3 min) and pressure of the carrier Oxygen gas (1.5 bar) were kept constant for each concentration. The prepared films was treated at (550 ºC) for 2 h. The X-ray diffraction patterns for the prepared films were obtained in a (Shimadzu XRD-6000)
goniometer using copper target (CuKα1, 1.5416 Å) .

3. RESULTS AND DISCUSION

Structural analysis

The X-ray diffraction pattern before and after annealing for the undoped and Vanadium doped SnO_2 deposited at (400 ^oC) are shown in Fig. (1) and Fig.(2). The diffraction peaks (110), (101), (200), which is in agreement with the Joint Committee of Powder Diffraction Standards (JCPDS card number (41-1445) with a tetragonal unit cell showing a preferred orientation along (110), and doping with V led to an decrease in the intensity of the diffraction peaks.

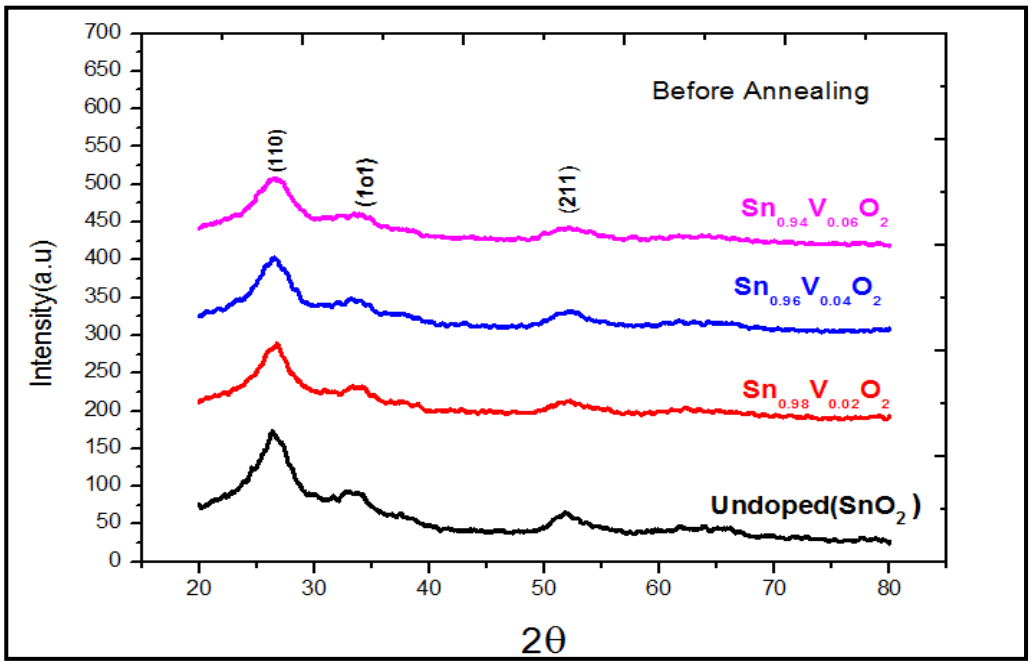

Fig.(1) X-ray diffraction pattern for the undoped and V doped SnO_2 before annealing

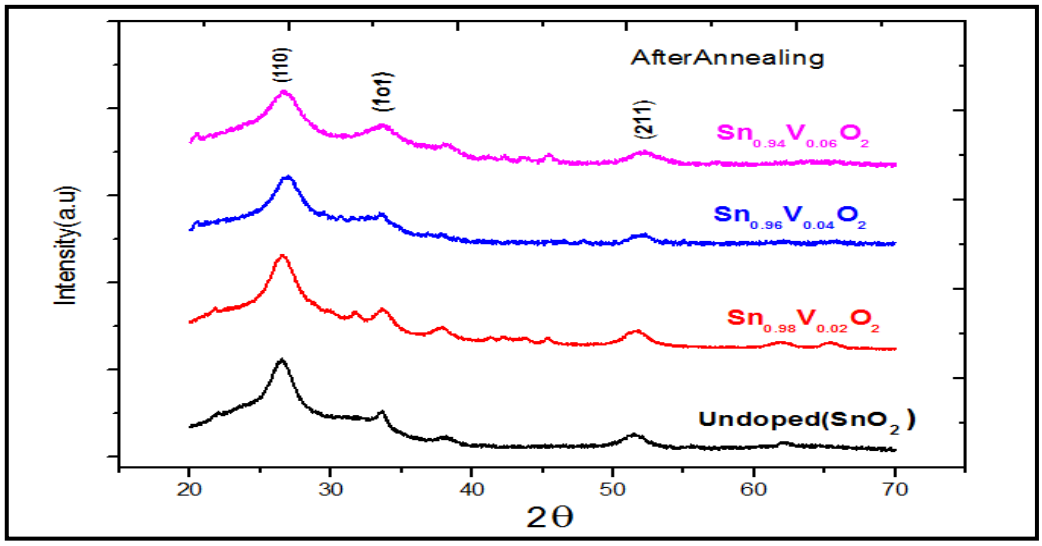

Fig.2 X-ray diffraction pattern for the undoped and V doped SnO_2 after annealing

(3-1) The average crystallite size

The average crystallite size for the films can be calculated for (110) direction by
Scherrer formula by using the relation [8]:

$D = K\lambda / \beta \cos\Theta$.....(1)

It is observed that the crystallite size for the Tin Oxide thin films from the (110) peaks decrease when ratio of doping by Vanadium increase, and the range of average crystallite size (4.54 - 2.68) nm before annealing and (4.60 - 3.78) nm after annealing as shown in Figure(3). The decrease of average crystallite size in our samples shows that at least a small quantity of V^{4+} ions substituted the Sn ions, since the V^{4+} ionic radius (0.58 Å) is smaller than that corresponding to Sn^{4+} ion (0.71 Å)[9]. as shown in Table (1).

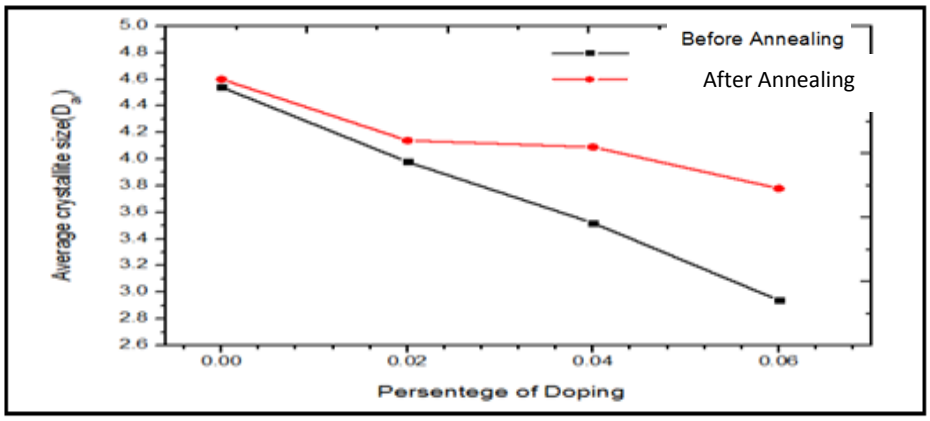

Fig.3 shows Average crystallite size as function of percenteg of doping before and after annealing

Table 1. Structural parameters of V-doped Tin Oxide thin films before and after annealing .

Sample		SnO_2 Undoped	$Sn_{0.98}V_{0.02}O_2$	$Sn_{0.96}V_{0.04}O_2$	$Sn_{0.94}V_{0.06}O_2$
hkl	Before	1 1 0	1 1 0	1 1 0	1 1 0
	After	1 1 0	1 1 0	1 1 0	1 1 0
2θ (deg)	Before	26.367	26.528	26.528	26.329
	After	26.511	26.511	26.904	26.676
d hkl (A)	Before	3.3770	3.35728	3.358	3.382
	After	3.359	3.354	2.916	3.339
FWHM(deg)	Before	1.80	2.05	2.32	2.78
	After	1.77	1.971	2.00	2.163
D_{av}	Before	4.54	3.98	3.52	2.94
	After	4.60	4.14	4.09	3.78
δ (nm^{-2})	Before	0.0485	0.0631	0.0807	0.1156
	After	0.0472	0.0512	0.0598	0.699

N_o (nm^{-2})	Before	4.2745	6.2344	9.1232	15.7404
	After	4.1100	5.637	5.846	7.406
$T_{c(hkl)}$	Before	1.6949	1.796	1.807	1.724
	After	1.280	1.417	2.006	1.736
Lattice constant (a_o)	Before	4.776	4.748	4.748	4.783
	After	4.188	4.216	4.850	4.235
Lattice constant (c_o)	Before	3.167	3.154	3.154	3.205
	After	5.625	5.538	5.955	5.423

(3-2) The lattice constants (a_o, c_o)

The lattice constants (a_o, c_o) for the films can be calculated as the following [10]:

$$\frac{1}{d^2} = \frac{h^2+k^2}{a_o^2} + \frac{l^2}{c_o^2} \quad \text{.....} (2)$$

The lattice constants(a_o) calculated for (110) direction and (c_o) calculated for (101) direction. All values of the lattice constants decrease when ratio of doping by vanadium increase, and the range of lattice constant (a_o) is (4.748- 4.776) nm before annealing and (4.188- 4.850) nm after annealing and the range of lattice constant (c_o) is (3.154- 3.205) nm before annealing and (5.423- 5.955) nm after annealing .

(3-3) Texture coefficient $T_c(hkl)$

The texture coefficient (*Tc*) represents the texture of a particular plane, in which greater than unity values imply that there are numerous of grains in that particular direction. The texture coefficients *Tc*(*hkl*) for all samples have been calculated from
the X-ray data using the well-known formula [11]:

$$T_C(hkl) = \frac{I(hkl)/I_0(hkl)}{N^{-1}\sum I(hkl)/I_0(hkl)} \quad \text{.....} (3)$$

where I(hkl) is the measured intensity, $I_o(hkl)$ taken from the JCPDS data, (*N)* is the
eflection number and (*hkl*) is Miller indices. The texture coefficient is calculated for crystal plane (110) of the undoped and V- doped SnO_2 films before and after annealing. All values of texture coefficient were

greater than 1 which indicates the abundance of grains in the (110) direction.

(3-4) Dislocation Density (δ)

The dislocation density is the measure of amount of defects in a crystal. The dislocation density (δ) can be calculated as the following [12]:

$\delta = 1/D_{av}^2$ .....(4)

The small value of dislocation density obtained in the present work confirmed good crystallinity of the ($Sn_{1-x}V_xO_2$) thin films fabricated by employing spray pyrolysis technique. Dislocation density increase when ratio of doping by V decrease, and the range of dislocation density (0.0485-0.1156) nm before annealing and (0.0472 - 0.699) nm after annealing as shown in tabl.(1).

(3-5)The Number of crystals (N_o)

The number of crystals per unit area can be calculated as the following[13]:

$N_o = t/ D_{av}^3$ .....(5)

Where t : is the thickness and N_o: is the number of grains It can be seen that the number of crystals of prepared films have values in the range of (4.2745-15.7404nm^{-2}) before annealing and (4.1100- 7.406 nm^{-2}) after annealing as shown in tabl.(1).

(3.6) Specific Surface Area (SSA)

SSA is the area per unit mass, it is factor to determines bulk rates of such reactions (unit m^2/g) [14]. It is very important in the nanoparticles because their large surface to volume ratio with a decrease in particle size[15]. SSA used in materials to determine their types and properties and is also used in case of reactions on surfaces, heterogeneous catalysis and adsorption[16].

Mathematically, SSA can be determined by using the relation(6) [17]. Specific surface area for undoped and V doped SnO_2 is shown in table (2).

$SSA=6 * 10^3 / D. \rho$ .....(6)

Where : SSA is the specific surface area and ρ is the density for undoped and

V doped SnO_2.

Table (2): Specific surface area for undoped and V doped SnO_2 before and after annealing.

Sample	ρ ($g.cm^{-3}$)	D_{av} (nm)		SSA ($m^2.g^{-1}$)	
		Before	After	Before	After
Undoped-SnO_2	6.95	4.54	4.6	188	187
$Sn_{0.98}V_{0.02}O_2$	6.87814	3.98	4.14	219	210
$Sn_{0.96}V_{0.04}O_2$	6.80628	3.52	4.09	250	215
$Sn_{0.94}V_{0.06}O_2$	6.73442	2.94	3.78	303	235

From table (2) it shows that SSA increases when the particle size decreases because of the particle diameter decreased.

4. Conclusions

We have synthesized $Sn_{1-x}V_xO_2$ with (x = 0, 0.02, 0.04, 0.06) and (0.08). The Influence of the doping degree on XRD of these Thin films was investigated.

The XRD results showed that all films are polycrystalline in nature with tetragonal structure and preferred orientation along (110) plane before and after annealing. The intensity of peaks was decrease with increasing of doping, The crystallite size and lattice constants was decrease with increasing of doping, While dislocation density, number of crystal and Specific Surface Area were increase with increasing of doping before and after annealing.

5- REFRENCES

[1] C. Wang, X. F. Chu, M. M. Wu, **"Highly sensitive gas sensors based on hollow sphere template method"** *Sensors and Actuators B*, Vol.120, No.508, (2007)

[2] S. C Ray, M. K. Karanjai, D. Dasgupta, , **"Tin dioxide based transparent semicondacting films deposited by dip-coating techingue"**, Surface & Coatings Technol,Vol.73,No.102, (1998).

[3] L.A.Patil**, "Ultrasonically sprayed nanostructured SnO_2 thin films for highly sensitive hydrogen sensing"**, ISBN 978-1-4398-34015 Vol.(1), 2010.

[4] A. J. Freeman, K. R. Poeppelmeirer, T. O. Mason, R. P. H. Chang, and T. J. Marks,**"Chemical and Thin-Film Strategies for New Transparen Conducting Oxides",** MRS Bull,Vol.25, No.45, (2000).

[5] James E. House Kathleen A. House" **Descriptive Inorganic Chemistry"** Illinois Wesleyan University Bloomington, Illinois, (2010).

[6] K.L. Chopra & I. Kaur, **"Thin Film Device Applications"**, Plenum prss, New York, 1983.

[7] R.R. Moskalyk a, A.M. Alfantazi b, "**Processing of vanadium: a review"**, Minerals Engineering,Vol.16,p.p (793–805),(2003).

[8] M. Caglar, S. Ilcan, Y. Caglar, **"Influence of Substrate Temperature on Structural and Electrical Properties of ZnO Films "**, J. Sci, Vol.7,No(2), p. p(153), (2006).

[9] A. Popa, D. Toloman, O. Raita, M. Stan, O. Pana**,"Ferromagnetic Behaviour of Vanadium Doped SnO_2 Nanoparticles and Nealed at Different Temperatures"**, Journal of Alloys and Compounds,Vol.591,p.p(201-206),(2014).

[10] P.Mitra, Khan, **"Chemical deposition of ZnO films from ammonium zincate bath"**,Materials Chemistry and Physics,Vol.98,P.279,(2008)

[11] C. Barret and B.T.Massalki**,"Structure of Metals"**Book,Oxford Pergamon, (1980).

[12 S.Ilican, Y.Caglar, M.Caglar, and F.Yaku phanoglu,**"Structural, optical and electrical properties of F-doped ZnO nano rod semiconductor thin films deposited by sol-gel process"**, Applied Surface Science, Vol. 255, p.p (2353-2359), (2008).

[13] C.Mwolfe, N.Holouyak, G.B.Stillmau**,"Physical Properties of Semiconductor"**, Printice Hall,New York (1989).

[14] M. E. Nielsen and M. R. Fisk**,"specific surface area and physical properties of subsurface basalt samples from the east flank of Juan de Fuca Ridge"** , Proceedings of the Integrated Ocean Drilling Program, No.301 (2008).

[15] A. Rahdar, V. Arbabi, and H. Ghanbari, **"Study of electro-optical properties of ZnS nanoparticles prepared by colloidal particles method"**, Int. J. of Chemical and Biological Engineering,V.6

[16] T. Theivasanthi and M. Alagar**, "Konjac biomolecules** (2012). **assisted–rod/ spherical shaped lead nano powder synthesized by electrolytic process and its characterization studies"**, Nano Biomed. Eng. Vol.5, pp. 11-19. (2013).

[17] T. Theivasanthi and M. Alagar, **"Electrolytic synthesis and characterization of silver nanopowder"**, Nano Biomed. Eng. Vol.4, pp. 58-65,(2012).